FORM and FORCE

Proceedings of the IASS Annual Symposium 2019 — Structural Membranes 2019
Form and Force
7—10 October 2019, Barcelona, Spain
C. Lázaro, K.-U. Bletzinger, E. Oñate (eds.)

Calculation of static deformation of membrane structures under the load of ponding water

Navaneeth K. Narayanan[*,b], **Roland Wüchner**[b] **and Joris Degroote**[a,c]

[*] Department of Flow, Heat and Combustion Mechanics, Ghent University
Sint-Pietersnieuwstraat 41, 9000 Ghent, Belgium
navaneeth.kodunthirappullynarayanan@ugent.be

[a] Department of Flow, Heat and Combustion Mechanics, Ghent University
[b] Chair of Structural Analysis, Technical University of Munich
[c]Flanders Make, Belgium

Abstract

Ponding refers to a phenomenon of accumulation of water on top of a structure. Even though most light weight membrane structures are designed to prevent its occurrence, it can be initiated in some cases during rainfall by an event such as drifted snow settling on the surface of the structure causing a local depression of the membrane structure. The present work proposes a method to calculate the static deformation of a membrane structure due to a given volume of ponding water. The method involves coupling of a structural solver for the membrane and a volume conserving solver representing the static behavior of an incompressible fluid. The coupling is performed in a partitioned manner with the linearized behavior of the incompressible fluid incorporated in the structural equations to accelerate the coupling iterations. Using this method, the final deformation of the structure due to ponding is calculated by applying loads due to a fixed volume of water.

Keywords: ponding, partitioned coupling, volume conserving solver, hydrostatic load

1 Introduction

Membrane structures are very efficient in carrying loads compared to the materials usage, but these structures undergo significant surface movement when loaded, making them vulnerable to the formation of a water pond. Rainfall along with an event such as snow settling or some dead loads on the structure can trigger accumulation of water in local depression. If the structure is not stiff enough this can cause more deflection leading to more ponding and so on. This cycle of increasing deformation and water accumulation may increase the load indefinitely resulting in structural collapse or failure. For the cases where the structure is much stiffer with good draining characteristics, the excess water will drain, resulting in a stable pond. However, even in this case if the rain is accompanied by strong winds, the wind flow around the structure may induce large oscillations. In 2011, during the Pukkelpop festival held in Kiewit (Belgium), a strong wind interacting with ponding water led to huge swaying of tents eventually resulting in the collapse of the structure. Studying such cases will involve fluid structure interaction (FSI) simulation between the membrane structure, the ponding water and the wind flow.

In order to simulate such systems it is necessary to find the static deformation of the membrane structure under the load of the ponding water. This will be the pre-processing step for the FSI simulation. The other applications of this analysis include floating caps of oil storage tanks [9], and optical reflector forming using ponding loads [7]. Some of the older works on studying the ponding on membranes include the work of Szyszkowski and Glockner [8] who studied ponding stability and deformation on spherical inflatables, where they solved axi-symmetric membrane equations with the hydrostatic loads. Tuan [7] focused on large deformations and strains of initially flat, simply supported circular membranes under gradually accumulated fluid pressure. He used fourth-order Runge-Kutta numerical integration with an iterative finite element analysis using shell elements to calculate the deformation due to the ponding. However, these studies only involved axi-symmetric geometries. One example of a general approach is presented in the work of Bown *et al.* [3], where an in-house structural code inTENS is coupled with a shallow water solver in a partitioned method to analyse ponding on tensioned membrane structures.
The idea presented in the current work is similar to Bown *et al.*, except here a volume conserving solver is used instead of a transient shallow water solver. The volume conserving solver conserves the given volume of incompressible fluid with a constraint that the top surface is normal to gravity, thus representing the free surface of the fluid in static condition. The coupling iterations are accelerated by adding the linearized static behaviour of the fluid under gravity in the structural solver. In terms of implementation this will translate into adding the load stiffness matrices to the tangent stiffness matrix of the membrane elements and a linear update of the top surface in the non-linear iterations of the structural solver. The required load stiffness matrices are mentioned shortly in the later sections but this has been extensively discussed in [1, 2], where the authors derive all the tangent stiffness matrices from the principle of virtual work. In each coupling iteration, hydrostatic load is applied on the structure based on the plane's height and the volume-conserving solver updates the plane's height depending on the deformation of the structure in order to conserve a given volume of water. When the convergence is achieved in the partitioned iterations, the deformed shape of the structure is determined. The following sections discuss the proposed volume-conserving solver and how it is coupled to a structural solver in KRATOS [4], an open-source finite element framework. At the end, an example is presented where the static deformation of the membrane structures is calculated due to the accumulation of an incompressible fluid.

2 Mathematical models

2.1 Hydrostatic load

Consider a membrane surface denoted by $\partial\Omega_s$ containing a certain volume of incompressible fluid. The free surface of the fluid, denoted by $\partial\Omega_f$ is perpendicular to gravity. The wetted region of the membrane, $\partial\Omega_{fs}$ experiences hydrostatic pressure proportional to the height of the free surface from the fluid above. If the gravity is along the z-direction then mathematically, the traction at a point P with z-coordinate, z on the structure can be stated as:

$$\begin{aligned} \mathbf{t} &= -\gamma_f(z - z_f)\mathbf{n} && \partial\Omega_{fs} \\ \mathbf{t} &= \mathbf{0} && \partial\Omega_s \setminus \Omega_{fs} \end{aligned} \tag{1}$$

where, z_f is the z-coordinate of the free surface, γ_f is the specific weight of the fluid, $\mathbf{n}$ is the outward unit normal vector at the point P. Figure 1 clearly indicates the symbols and terminologies used.

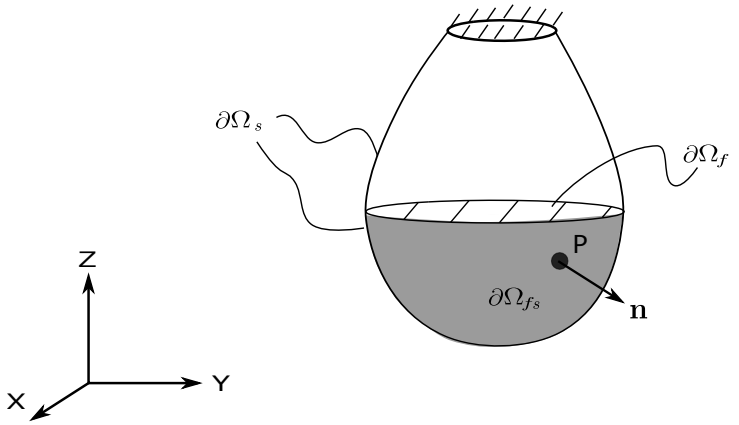

Figure 1: Hydrostatic loading by a fluid on a membrane.

2.2 Structural equations

the variational formulation of the static non-linear membrane in its reference configuration can be written as

$$-\int_{\partial\Omega_s^0} h\ \mathbb{S} : \delta\mathbb{E}\ dS + \int_{\partial\Omega_s^0} \mathbf{t}_0 \cdot \delta\mathbf{u}\ dS = 0, \tag{2}$$

where $\mathbb{S}$ and $\mathbb{E}$ are the second Piola-Kirchhoff stress tensor and the Green-Lagrange strain tensor, respectively. The first term in the equation 2 is the virtual internal work (δW_{int}) and the second term is the external virtual work (δW_{ext}), corresponding to the virtual displacement $\delta\mathbf{u}$. With the assumptions of large displacement and small strains, we only consider the Saint-Venant Kirchhoff material law, equation 3, in the numerical example presented in this paper.

$$\mathbb{S} = 2\mu\mathbb{E} + \lambda\mathbb{E} : \mathbb{I} \tag{3}$$

The tangent stiffness matrix of the membrane elements ($\mathbb{K}_{mem}$) can be obtained by discretising equation 2 and deriving δW_{int} by the nodal displacement vector $\hat{\mathbf{u}}$. For more details on the derivation of membrane elements, please refer to [10]. For the case of hydrostatic loading, δW_{ext} can be written in the current configuration by using equation 1 giving

$$\begin{aligned}\delta W_{ext} &= \int_{\partial\Omega_{fs}} \delta\mathbf{u} \cdot p\mathbf{n} ds \\ &= -\int_{\partial\Omega_{fs}} \delta\mathbf{u} \cdot \gamma_f(z - z_f)\mathbf{n} ds.\end{aligned} \tag{4}$$

In the equation 4, the external work term is calculated based on z_f determined by the volume conserving solver. By linearizing the discretized form of equation 4 and subtracting it from the membrane tangent stiffness matrix the convergence speed of the coupling iterations between the structural and the volume conserving solver can be improved. Even though, the free surface is moved by the volume conserving solver in every coupling iteration to conserve a given volume of water, the water level should also change during the non-linear iterations of the structural

solver. This is not directly performed by the volume conserving solver as it was found to be unstable in some numerical experiments. Actually, if the volume conserving solver was used in structural iterations, the external coupling iterations is not required and the convergence will be much faster. But for the algorithm to be more robust, it was decided to perform the coupling external to the structural solver with the linear update of the free surface inside the non-linear iterations of the structure, given by

$$Dz_f[\mathbf{u}] = \Delta z_f = \frac{-\int_{\Omega_{fs}} \Delta\mathbf{u}\cdot\mathbf{n}\ ds}{A_f}. \tag{5}$$

The linearization of the external work term from the hydrostatic pressure in the equation 4 is given by

$$\begin{aligned} D\delta W_{ext}[\mathbf{u}] = &-\gamma_f \int_{\partial\Omega_{fs}} \delta\mathbf{u}\cdot Dz[\mathbf{u}]\ \mathbf{n}\ ds + \gamma_f \int_{\partial\Omega_{fs}} \delta\mathbf{u}\cdot Dz_f[\mathbf{u}]\ \mathbf{n}\ ds \\ &-\gamma_f \int_{\partial\Omega_{fs}} \delta\mathbf{u}\cdot(z-z_f)\ D\mathbf{n}[\mathbf{u}]\ ds. \end{aligned} \tag{6}$$

Substituting $Dz[\mathbf{u}]$ from equation 5 we get

$$\begin{aligned} D\delta W_{ext}[\mathbf{u}] = &-\gamma_f \int_{\partial\Omega_{fs}} \delta\mathbf{u}\cdot Dz[\mathbf{u}]\ \mathbf{n}\ ds - \frac{\gamma_f}{A_f}\left(\int_{\partial\Omega_{fs}} \delta\mathbf{u}\cdot\mathbf{n}\ ds\right)\left(\int_{\partial\Omega_{fs}} \Delta\mathbf{u}\cdot\mathbf{n}\ ds\right) \\ &-\gamma_f \int_{\partial\Omega_{fs}} \delta\mathbf{u}\cdot(z-z_f)\ D\mathbf{n}[\mathbf{u}]\ ds. \end{aligned} \tag{7}$$

Discretizing equation 7 using the shape functions matrix $\mathbb{N}$ and the nodal displacement vector $\hat{\mathbf{u}}$, we can write the equation 7 in terms of the load stiffness matrix $\mathbb{K}_p$, the incremental nodal displacement vector $\Delta\hat{\mathbf{u}}$ and the virtual displacement $\delta\hat{\mathbf{u}}$. The discretized equation for each membrane element inside the wetted region Ω_{fs} is given in equation 8, which is assembled in a global matrix to give $\mathbb{K}_p$.

$$\begin{aligned} D\delta W^e_{ext}[\mathbf{u}] =&\delta\hat{\mathbf{u}}^{eT}\left\{-\gamma_f \int_\xi\int_\eta \mathbb{N}^T\tilde{\mathbf{n}}\mathbf{e}_z^T\mathbb{N}\ d\xi d\eta - \frac{\gamma_f}{A_f}\left(\int_\xi\int_\eta \mathbb{N}^T\tilde{\mathbf{n}}\ d\xi d\eta\right)\left(\int_\xi\int_\eta \tilde{\mathbf{n}}^T\mathbb{N}\ d\xi d\eta\right)\right. \\ &\left.-\gamma_f \int_\xi\int_\eta (z-z_f)\left(\mathbf{g}_\xi\times\frac{\partial\mathbb{N}}{\partial\eta} - \mathbf{g}_\eta\times\frac{\partial\mathbb{N}}{\partial\xi}\right)\ d\xi d\eta\right\}\Delta\hat{\mathbf{u}}^e \\ =&\delta\tilde{\mathbf{u}}^T\mathbb{K}^e_p\Delta\tilde{\mathbf{u}}^e \end{aligned} \tag{8}$$

with the corresponding virtual external work for each element,

$$\begin{aligned} \delta W^e_{ext} &= -\delta\hat{\mathbf{u}}^{eT}\gamma_f \int_\xi\int_\eta \mathbb{N}^T(z-z_f)\tilde{\mathbf{n}}\ d\xi d\eta \\ &= \delta\hat{\mathbf{u}}^{eT}\mathbf{F}^e_p \end{aligned} \tag{9}$$

In equation 8 and 9, the integration is performed in the parametric domain, where the unit normal vector $\mathbf{n}$ is replaced by the normal vector $\tilde{\mathbf{n}}$ using the relation, $\mathbf{n}\ ds = \tilde{\mathbf{n}}\ d\xi d\eta$. In equation 8, $\mathbf{g}_\xi$ and $\mathbf{g}_\eta$ are the basis vectors at any point in the element. In the current work, only constant strain triangle (CST) elements are considered with the numerical integration based on Gauss quadrature. For the elements that are cut by the free surface the integration is performed by dividing the cut triangles and performing Gauss integration on the triangles that are below the free surface, as shown in the figure 2. The final equation after the assembly for arbitrary $\delta\tilde{\mathbf{u}}$ is solved in every non-linear iteration of the structure, until convergence, giving

$$\begin{aligned} &\delta\tilde{\mathbf{u}}^T \left(\mathbb{K}_{mem} - \mathbb{K}_p\right) \Delta\tilde{\mathbf{u}} = \delta\tilde{\mathbf{u}}^T \left(\mathbf{F}_p - \mathbf{F}_{mem}\right) \\ \implies &\left(\mathbb{K}_{mem} - \mathbb{K}_p\right) \Delta\tilde{\mathbf{u}} = \mathbf{F}_p - \mathbf{F}_{mem} \end{aligned} \tag{10}$$

where $\mathbf{F}_{mem}$ is the global internal force vector of the membrane. In each non-linear structural iteration the global hydrostatic force vector $\mathbf{F}_p$ is calculated based on the position of the free surface which is updated according to equation 5.

3 Volume conserving solver

The volume conserving solver consists of two components: a volume calculation algorithm and a iterative algorithm to conserve a given volume. The volume of $\partial\Omega_{fs}$ in figure 1 can be calculated using the relation,

$$V_f = \int_{\partial\Omega_s} (z - z_f)\mathbf{e}_z \cdot \mathbf{n} ds \tag{11}$$

and its derivative with respect to z_f,

$$\frac{\partial V_f}{\partial z_f} = \int_{\partial\Omega_s} -\mathbf{e}_z \cdot \mathbf{n} ds = A_f \tag{12}$$

where A_f is the area of the free surface. The integration in equation 11 and 12 is performed numerically using Gauss quadrature, in the same way as explained in the previous section. In the current work, leap-frogging Newton's method is used for conserving a given volume. This method is discussed in detail in [6]. It consists of a Newton step followed by a pseudo secant step. The main advantage of this method is that it only involves one derivative evaluation, like Newton's method and yet it can attain cubic convergence. The Newton method and leap-frogging method were tested for volume conservation with a complicated geometry and it was found that the leap-frogging Newton was much more robust and had faster convergence rate than Newton's method. Hence, it was chosen over the other. The equation used for iteration to conserve the volume is given in equation 13, with the function f and x_n being the difference between the current volume and the target volume $(V_f^n - V_t)$, and the z-coordinate of the free surface at the n^{th} iteration, respectively. The derivative of function, f' is given by equation 12, which is the area of the free surface at the n^{th} iteration.

$$\begin{aligned} \tilde{x}_n &= x_n - \frac{f(x_n)}{f'(x_n)} \\ x_{n+1} &= x_n - \frac{f(x_n)^2}{f'(x_n)\left(f(x_n) - f(\tilde{x}_n)\right)} \end{aligned} \tag{13}$$

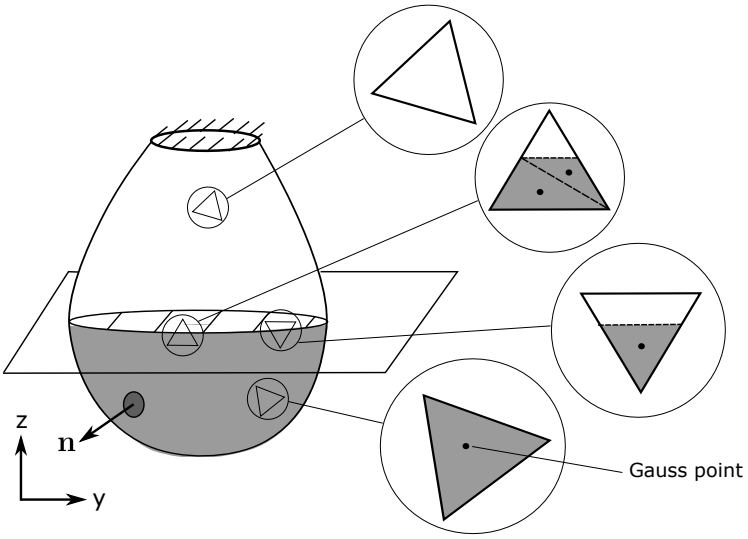

Figure 2: Gauss integration in the wetted region.

4 Partitioned coupling

The static structural deformation under the load of a given volume of fluid, V_t is obtained when the variational equation of the structure, equation 2, and boundary conditions given in equation 1 are satisfied with fluid volume $V = V_t$. The solution of the problem is obtained by iterating between structural solver and volume-conserving solver until the norm of the displacement change between the iterations is under a certain tolerance. Because the linearized part of the fluid is added in the structural system, there was no need to use any convergence accelerators like Aitken or IQNLS [5]. This claim is also supported by the numerical experiments that were carried out. For example, in the numerical example presented in the paper, for most of the fluid volume the number of coupling iterations was around 3 or 4.

5 Numerical example: Ponding on a pnuematic membrane structure

Before performing the simulation of this case, the volume conserving solver was validated with a known case where the enclosed volume was already known. The partitioned coupling between the solvers was also validated with the numerical results presented in table 2 of [7]. Here, the maximum vertical displacements corresponding to four different fluid volumes were compared and were found to be in very close agreement. In the numerical example presented in this paper, we consider an inflated thin-walled membrane hemisphere with Young's modulus $E = 7 \times 10^6\ N/m^2$, Poisson ratio $\nu = 0.45$ and thickness $t = 0.002\ m$. A difference in pressure of $p = 0.5\ kPa$ compared to the atmospheric pressure is applied at the internal surface. To get the perfect hemisphere of diameter $D = 10\ m$ after the application of pressure, an isotropic normal pre-stress calculated from the formula $\sigma_{mem} = pD/4t = 1.2MPa$ is applied on the membrane with zero shear stress. The hemisphere is clamped at the bottom boundary and for reducing the computational time only a quarter section of the hemisphere is simulated considering the symmetry of the problem. To start the ponding process, we first apply a dead load of $w = 1\ kPa$ on the top surface of the membrane enclosed by a circle of radius $R_{dead} = 1.736\ m$ as a seed event. Due to the dead load, there will be a local depression in the hemisphere. In

the created depression, a hydrostatic load due to different volumes of water was applied. The results are obtained by running the partition coupling iterations with various target volumes as input in the volume conserving solver. In all the simulations considered in the example, the volume conserving solver is initialized from the topmost point of the undeformed hemisphere. The vertical displacements of top most point of the hemisphere corresponding to the different fluid volumes are given in table 1. Figure 3 shows the deformed shape of a cut section of the hemisphere for $V_t = 1.6\ m^3$. The distance from the free surface is scaled to positive and negative values very close to zero to show the wetted surface of the hemisphere.

Table 1: Vertical displacement of the top most point of the hemisphere (u_z) and vertical position of the free surface (z_f) for different volume of water (V_t).

$V_t\ [m^3]$	0.0	0.8	1.6	2.4	3.2	4.0
$u_z\ (m)$	-0.972	-2.442	-3.709	-4.950	-6.214	-7.531
$z_f\ (m)$	N.A.	7.986	6.950	5.887	4.774	3.590

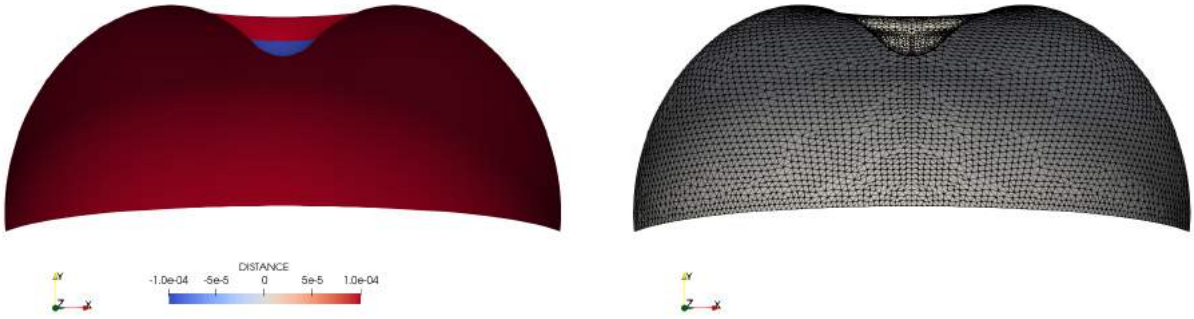

(a) Distance from the free surface.

(b) Deformed geometry with mesh.

Figure 3: Deformed geometry of inflated the hemispherical membrane due to the ponding of water with $V_t = 1.6\ m^3$.

6 Conclusion and Outlook

An algorithm for calculating the static deformation of a structure due to ponding load from a fixed volume of fluid was developed. The algorithm involved partitioned coupling of a structural solver and a volume conserving algorithm, responsible for maintaining a constant volume of fluid on the structure. The linearized contribution of the fluid behavior was added in the structural iterations to accelerate the coupling. The obtained deformation will be used as the initial condition for the FSI simulation of the membrane structure, ponding water and wind flow.

7 Acknowledgements

The authors gratefully acknowledge the funding of the Research Foundation – Flanders (FWO) for this work (project number G086517N).

References

[1] T. Rumpel and K. Schweizerhof, "Hydrostatic fluid loading in non-linear finite element analysis," *International Journal for Numerical Methods in Engineering*, vol. 59(6), pp. 849-870, 2004.

[2] C. Hoareau and J.-F Deü. "Non-linear finite element analysis of an elastic structure loaded by hydrostatic follower forces," *Procedia Engineering, Elsevier*, vol. 199, pp. 1302-1307, 2017.

[3] A. Bown, T. Makin and D. Wakefield, "Beyond Static Analysis: Investigation of Membrane Structure Performance Using Time Stepping, Transient and Progressive Analyses," *Procedia Engineering*, vol. 155, pp. 1877-7058, 2016.

[4] P. Dadvand, R. Rossi and E. Oñate, "An object-oriented environment for developing finite element codes for multi-disciplinary applications, "Archives of computational methods in engineering," vol. 17(3), pp. 253–297, 2010.

[5] J. Degroote, "Partitioned Simulation of Fluid-Structure Interaction." *Archives of Computational Methods in Engineering*, vol. 20(3), pp. 185-238, 2013.

[6] J.B. Kasturiarachi, "Leap-frogging Newton's method," *International Journal of Mathematical Education in Science and Technology*, vol. 33(4), pp. 521-527, 2002.

[7] C. Y. Tuan, "Ponding on circular membranes" *International journal of solids and structures*, vol. 35, pp. 269-283, 1998.

[8] W. Szyszkowski and P. Glockner "Finite deformation and stability behaviour of spherical inflatables subjected to axi-symmetric hydrostatic loading" *International journal of solids and structures*, vol. 20, pp. 1021-1036, 1984.

[9] H. I. Epstein and T. J. Strnad, "Liquid-filled, liquid-supported, circular structural membranes," *Computers & structures*, vol. 21, pp. 443-451, 1985.

[10] R. L. Taylor, E. Onate, P. -A. Ubach, "Finite element analysis of membrane structures" *Textile composites and inflatable structures*, pp. 47-68, 2005.